Received: 6 January 2019 | Revised: 6 March 2019 | Accepted: 12 March 2019

DOI: 10.1002/pip.3136

RESEARCH ARTICLE

WILEY PROGRESS IN PHOTOVOLTAICS

Solution-processed copper (I) thiocyanate (CuSCN) for highly efficient CdSe/CdTe thin-film solar cells

Angelique Montgomery[1] | Liping Guo[1] | Corey Grice[2] | Rasha A. Awni[2] | Swapnil Saurav[1] | Lin Li[1] | Yanfa Yan[2] | Feng Yan[1,3]

[1] Department of Metallurgical and Materials Engineering, The University of Alabama, Tuscaloosa, AL 35487

[2] Department of Physics and Astronomy, and Wright Center for Photovoltaics Innovation and Commercialization, University of Toledo, Toledo, OH 43606

[3] Center for Materials for Information Technology, The University of Alabama, Tuscaloosa, AL 35487

Correspondence
Yanfa Yan, Department of Physics and Astronomy, and Wright Center for Photovoltaics Innovation and Commercialization, University of Toledo, Toledo, OH 43606.
Email: yanfa.yan@utoledo.edu

Feng Yan, Department of Metallurgical and Materials Engineering, The University of Alabama, Tuscaloosa, 35487.
Email: fyan@eng.ua.edu

Abstract

Solution-processed CuSCN serving as hole transport, electron reflecting layer (HTL, ERL) and Cu dopant source for CdSe/CdTe thin-film solar has demonstrated high power conversion efficiency (PCE) of ~17%. Two types of solvent, diethyl sulfide (DES) and aqueous ammonia (NH_4OH), are explored to deposit CuSCN on CdTe, and both can enhance the performance of CdSe/CdTe solar cells. However, NH_4OH solvent is less toxicity, leading to a smoother surface than DES solvent, enabling the deposition of ultra-thin CuSCN layer and avoiding the high cost of DES. Temperature-dependent current-voltage (J-V-T) and capacitance-voltage (C-V-T) measurements reveal that the use of CuSCN HTL increases hole concentration in CdTe absorber and significantly reduces back-contact barrier height. High power conversion efficiency is achievable with the optimal thickness of the CuSCN layer. Our results demonstrate solution-processed CuSCN HTL for enhancing the efficiency and reducing the cost of CdTe thin-film solar cells.

KEYWORDS

CdTe photovoltaics, Cu doping, CuSCN, hole transport layer, solution process

1 | INTRODUCTION

CdTe is the most successful thin-film solar cells technology with certificated 22% record power conversion efficiency (PCE), dominating the thin-film solar cell markets due to its low cost, desired bandgap, high optical absorption coefficient, and stability in ambient.[1,2] Although Cd toxicity and Te limited reserves in the earth, CdTe is still the most affordable solar cells technology per the levelized cost of electricity (LCOE) price (~$0.04/kWh) while the national average LCOE from all sources[3] ~$0.11/kWh. To further reduce the electricity price (eg, ~$0.03/kWh), higher efficiency and lower cost of CdTe solar cell are demanded.[4] With the integration of a CdSe layer as the window layer for the CdTe device, the short-circuit photocurrent (J_{sc}) of CdTe has been improved to above 30 mA cm^{-2} by forming gradient absorber to absorb more sunlight in both short and long wavelength.[1,5] To further elevate the PCE of CdTe solar cells, higher open circuit voltage (V_{oc}) and fill factor (FF) are needed. Traditionally, to improve the V_{oc}, Cu doping is an affordable and an effective way during high-efficiency CdTe devices fabrication. Recently, considerable strategies have been proposed and demonstrated successfully to improve V_{oc}. For example, a higher open circuit voltage above 1.0 V in monocrystalline CdTe with PCE ~17% by doping phosphorus (P) has been achieved.[6] However, polycrystalline CdTe devices with 22% PCE suffers a relative low V_{oc} close[7] to 0.9 V. It is a huge challenge to introduce P or other group V dopants (eg, As and Sb) into the polycrystalline CdTe to further improve[8-10] the $V_{oc.}$

Thus, an alternative way to further enhance the V_{oc} is to apply the hole transport layer (and/or electron reflecting layer) to improve the carrier collection function.[11-14] Various inorganic and organic hole transport layers have been employed on CdTe devices to increase the hole extraction, such as Cu doped ZnTe, P3HT, PEDOT:PSS, and Sprio-OMeTAD.[15-18] However, depositing these functional layers may

Angelique Montgomery and Liping Guo contributed equally to this work.

need expensive physical vapor deposition facilities. To further reduce the cost of the solar cells, an affordable and effective solution process to integrate these functions in one layer (eg, hole transport layer, electron blocking layer, and doping) is desired.

Copper thiocyanate (CuSCN) is an inexpensive inorganic material with promising electronic property (eg, high work function ~5.3 eV) and optical properties (eg, bandgap ~3.6 eV), which has been investigated for several decades.[19,20] Recently, CuSCN as a promising and cost-effective hole transport layer for perovskite solar cells has achieved PCE ~20% using a solution-processed procedure.[21] Meanwhile, CuSCN was also used for other dye-sensitized solar cells (DSSC),[22,23] such as chalcogenides Sb_2S_3. As for CdTe solar cells, physical vapor deposited CuSCN thin film has also been investigated to improve the V_{oc} for CdS/CdTe devices.[24] Although, it is a challenge for solution-processed CuSCN (~100 nm) to achieve a thin layer compared with the vapor process counterpart (~10 nm) in CdS/CdTe devices. It is deserved to tailor the solution-processed CuSCN on CdTe devices considering that CuSCN uniquely combines desirable characteristics as Cu source for CdTe p-type doping, desired hole extraction, and electron reflecting behavior. In particular, an aqueous CuSCN solution for CdTe is even promising to be integrated into the ambient solution process for a high-throughput manufacturing. Traditionally, diethyl sulfide (DES) uses for dissolving CuSCN. However, the DES-based CuSCN layer is difficult to get an ultrathin and smooth layer due to the high viscosity and rougher topography of DES.[24,25] Recently, using aqueous ammonia (NH_4OH) as a solvent for CuSCN can achieve a relatively thin layer (5-10 nm) with smooth topography and successfully utilized on perovskite solar cells to obtain PCE ~17%.[26]

In this study, we applied solution-processed CuSCN as hole transport layer for the CdSe/CdTe thin-film solar with DES and aqueous NH_4OH as solvents, respectively. The improved V_{oc} and *FF* for the CdSe/CdTe solar cells with the solution-processed CuSCN lead to 17% PCE with reduced series resistivity by CuSCN thickness and concentration optimization. The improved device performance benefits from CuSCN for high V_{oc} and FF, while CdSe window layer accounts for high J_{sc} contributes the efficiency improvement. Temperature-dependent current-voltage and capacitance-voltage measurements reveal that the use of CuSCN HTL increases hole concentration in CdTe absorber can significantly reduce the back-contact barrier height. The CdTe devices with aqueous NH_4OH-based CuSCN solution show similar devices performance to that of DES-based CuSCN. The cost-effective solution-processed CuSCN for CdTe devices provides a promising pathway to reduce the cost of solar energy technology production.

2 | EXPERIMENTAL SECTION

2.1 | CuSCN solution preparation and deposition

CuSCN (99% Sigma-Aldrich) was dissolved into diethyl sulfide (98%, Sigma Aldrich) and aqueous ammonia (NH_4OH, 28% Alfa Aesar) at a concentration of 10 and 20 mg mL^{-1}, respectively. The solutions were magnetic-stirred at room temperature for 5 hours to get fully dissolved and filtered using a 0.45-μm pore size PTFE filter prior to the thin-film spin coating deposition. The CuSCN thin-film was deposited by spin coating with tunable rotation speed (1000 to 8000 rpm) to control the film thickness for 30 seconds.

2.2 | Solar cells fabrication

The CdTe film with ~3 μm was deposited on the sputtered CdSe (~100 nm) buffered F-doped SnO_2 (FTO, NSG USA) substrate using the close space sublimation (CSS). The detailed CSS deposition process was reported elsewhere.[5] The CdTe films were thermally treated using the $CdCl_2$ solution at 400°C for 20 minutes in the ambient. The CdTe surface was raising using the deionized water (DIW) to remove the residual $CdCl_2$, following an etching process using the diluted HCl solution to remove the surface oxides layer before the CuSCN coating and back contact deposition. For DES-based CuSCN, solution was denoted as DES-CuSCN, and for NH_4OH-based CuSCN, solution was denoted as NH-CuSCN. The thickness of the DES-CuSCN and NH-CuSCN layers was 30 to 60 nm and 10 to 20 nm respectively, tuned through the spin coater rotation speed. Thickness was measured using a Stylus profiler (Dektak II). The back contact for the CdTe cells was screen-printed graphite and Ag paste without intentional Cu source. The cells area is 0.08 cm^2. The cells were heat treated for about 20 minutes at 200°C to drive the Cu into the CdTe.

2.3 | Electrostatic surface characterization

The atomic force microscopy (AFM) and electrostatic force microscopy (EFM) were conducted using atomic force microscopy (AFM, Park XE70) using a Pt/Ir coated contact probe (ANSCM-PT from AppNano, Inc). The cantilever spring constant was about 3 N/m, and resonance frequency was ~60 kHz.

2.4 | Solar cell measurement and simulation

The current-voltage (*J-V*) curve of the solar cells was characterized using a solar simulator (Newport, Oriel Class AAA 94063A, 1000 Watt Xenon light source) with a source meter (Keithley 2420) at 100 m W cm^{-2} AM 1.5G irradiation. A calibrated Si-reference cell and meter (Newport, 91150 V, certificated by NREL) was used to calibrate the solar simulator prior to cells measurement. External quantum efficiency (EQE) data were characterized by a solar cell spectral response measurement system (QE-T, Enli Technology, Co Ltd). The solar cell device simulation was performed using the solar cell capacitance simulator (SCAPS) simulation.[27]

2.5 | Solar cell electrical characterization

Temperature-dependent current-voltage (J-V-T) and capacitance-voltage (C-V-T) measurements were performed using a Solartron

Modulab potentiostat equipped with a frequency response analyzer (Ametek Inc). The J-V-T measurements were performed in dark with DC voltage sweeping from −0.4 to 1.5 V. The C-V measurements were performed in the dark with a constant modulation voltage 45 mVrms and frequency of 10 kHz. AC signal superimposed on a DC bias voltage varying from −2.0 to 0.5 V. A liquid-nitrogen cooled cryogenic system (Janis VPF-100) was used to carry out all temperature dependent (150 to 300 K with a step size of 10 K) measurements. The temperature was controlled by a temperature controller (Lakeshore 330). A temperature sensor was mounted on the top of the device directly, to ensure that the recorded temperature is the device temperature.

3 | RESULTS AND DISCUSSION

3.1 | Solution selection for CuSCN

Figure 1A shows the energy level diagram of the FTO/CdSe/CdTe/CuSCN/graphite, where the CuSCN combines the hole transport layer and electron reflecting layer dual role based on the bandgap edge offset with respect to that of CdTe. Figure 1B indicates the bandgap diagram calculated using SCAPS modeling.[27] CuSCN thickness directly impacts the carrier transport due to its high resistivity and can play as a barrier for the carrier transport if the thickness is too thick.[24] Figure 1C shows the two solvents in this work to tune the thickness of CuSCN layer. The CuSCN powder dissolved into DES is transparent corresponding to its wide bandgap (~3.6 eV). While the CuSCN dissolved into NH_4OH solution is dark blue color, which is associated with the $(Cu(NH_4)_2)^+$ complex formation.[26,28,29] In both cases, the final CuSCN film (after extraction of the solvent) is transparent because of its large bandgap. The chemical structure of inorganic CuSCN is presented in Figure 1C, where the Cu ions are split by the SCN ions and a strong Cu—S bond that interconnects three-dimensionally. The structure also makes CuSCN a Cu source for CdTe Cu doping, which is a necessary process to improve the V_{oc} in CdTe devices.[30] Thus, CuSCN used for CdTe devices plays multiroles to engineer the device performance.

To understand the different interface quality and surface electronic behavior between the DES- and NH_4OH-based CuSCN on the CdTe surface, the atomic force microscopy (AFM) and electrostatic force microscopy (EFM) were carried out. The CuSCN layers were spin-coated on the etched CdTe surface. The bare CdTe surface without CuSCN as a reference is shown in Figure 2A, D for AFM morphology and EFM amplitude, respectively. The CdTe grain size is in the micrometer level (2-3 μm). In the EFM amplitude image, the grain boundary shows relative lower electrostatic force value compared with the grain, suggesting that the Cl passivation at the grain boundary after $CdCl_2$ heat treatment.[5] Figure 2B, E shows the AFM morphology and EFM amplitude images for the DES/CuSCN, respectively. The DES/CuSCN particles in nanoscale (~50-100 nm) can be observed with a surface root mean squared (RMS) roughness of ~7 nm (Figure 2B), which is consistent with the DES/CuSCN coated on the glass substrate.[26] The EFM images in Figure 2E show that the electrostatic force on the DES/CuSCN can significantly reduce the surface charges on the CuSCN. The electrostatic amplitude was reduced one order of magnitude (CdTe/CuSCN surface ~2 eV vs bare CdTe surface ~24 eV), as shown in Figure 2D, E, which suggests that the CuSCN layer is highly resistive and can prevent the electron transport through the back contact (ie, electron reflecting role). As shown in Figure 2C, F, the NH/CuSCN film is much smoother morphology with RMS ~1.2 nm than that of the DES/CuSCN, and the electronic surface is more uniform. This smoother surface of NH/CuSCN can planarize the rough bare CdTe surface and provide better contact with the back contact. Meanwhile, the NH/CuSCN film shows similar electronic behavior as that of the DES/CuSCN, also could reduce the reflecting the electron transport in the back contact. With the aqueous NH_4OH as a solvent for CuSCN, it is more convenient to tailor the thickness of CuSCN than that of DES solvent.

3.2 | DES/CuSCN impact on CdTe devices

Figure 3 shows the device performance for the DES-/CuSCN-based CdSe/CdTe solar cells with tuning the CuSCN thickness. It is reported

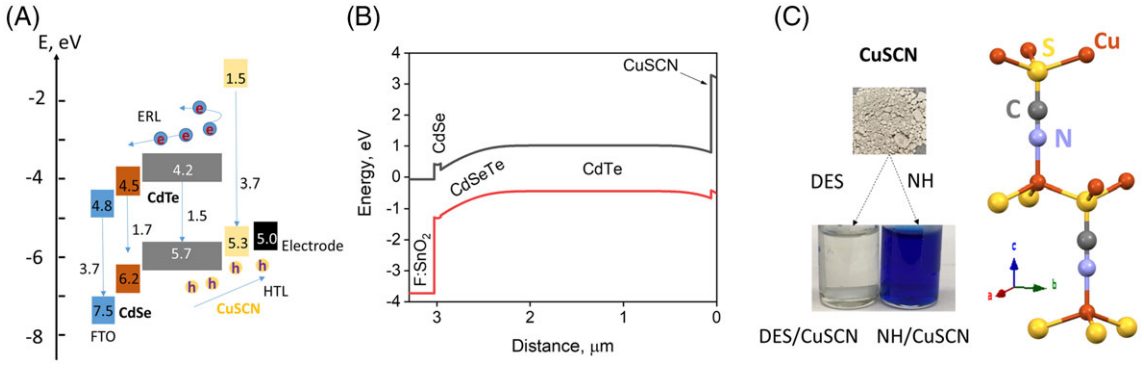

FIGURE 1 A, The energy level diagram of each layer in the FTO/CdSe/CdTe/CuSCN/graphite solar cells. B, SCAPS modeling determined energy band diagram of the solar cells. C, CuSCN powder dissolved into DES and NH_4OH, respectively. The CuSCN chemical structure is shown [Colour figure can be viewed at wileyonlinelibrary.com]

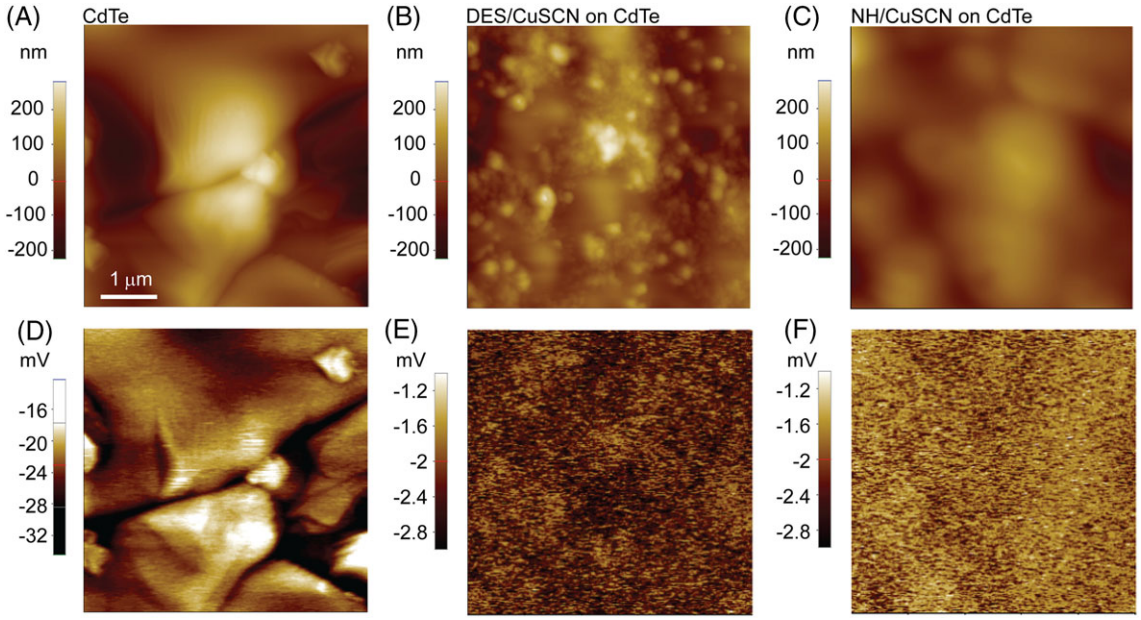

FIGURE 2 A, B, C, Atomic force microscopy (AFM) surface morphology images. D, E, F, Electrostatic force microscopy (EFM) amplitude images of bare CdTe, DES-/CuSCN-coated, and NH-/CuSCN-coated CdTe, respectively. (5 × 5 μm^2) [Colour figure can be viewed at wileyonlinelibrary.com]

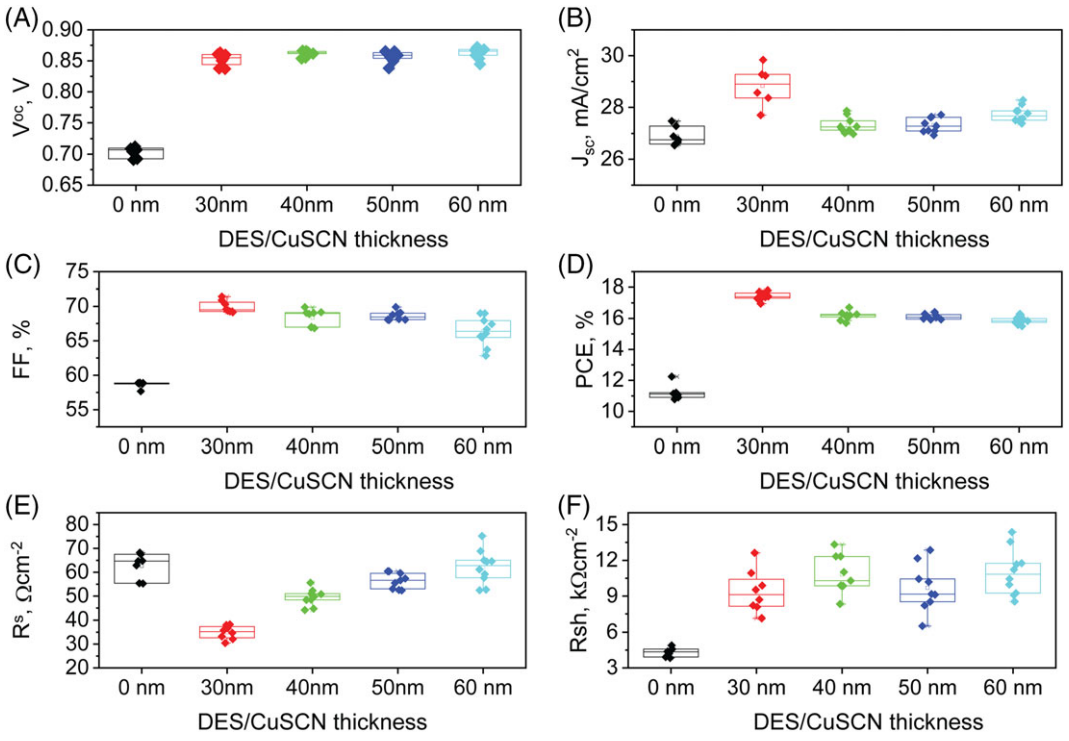

FIGURE 3 Statistical distribution of A, V_{oc}, B, J_{sc}, C, *FF*, D, PCE, E, R_s, and F, R_{sh} of CdTe solar cells based on CuSCN from DES solution. The cell performance data were selected for 10 cells for each CuSCN thickness [Colour figure can be viewed at wileyonlinelibrary.com]

that the sputtered CuSCN thickness can influence the CdS/CdTe devices performance remarkably, in particular, will improve the V_{oc}, and reduce the fill factor.[24] Without CuSCN (i.e., 0 nm, means no HTL, ERL, and Cu doping), the CdSe/CdTe device PCE is ~11%, V_{oc} ~0.7 V, J_{sc} ~26.5 mA cm^{-2}, and the Fill factor ~58%, which is similar to that of CdS/CdTe devices without CuSCN.[24] The improved J_{sc} compared with the CdS/CdTe device is due to the CdSe window layer can be consumed by CdTe to form into $CdSe_xTe_{1-x}$ absorber, which can absorb more short and long wavelength sunlight spectrum.[5,31] The dominated cause for the inefficient device performance is associated

with the high series resistivity (R_s) and low shun resistance (R_{sh}), as shown in Figure 3E, F, possibly due to the lack of Cu doping. With the introduction of CuSCN layer, the PCE of the CdSe/CdTe device can be boosted to 16% with 60 nm thick DES/CuSCN layer. The increase for the device parameters can reach V_{oc} ~0.855 V, and J_{sc} ~27.5 mA cm^{-2}, FF ~67%. This device performance improvement originates from the Cu doping effect from CuSCN. The incorporation of the CuSCN is also expected to be an electron reflecting layer due to its wide bandgap and high conduction band minimum (CBM), as shown in Figure 1A, B. However, the series resistance, R_s, is still high and similar to that of the CdTe without CuSCN. This is expected because the high resistivity of the thicker CuSCN layer prevents the carrier transport.[24]

Here, we tailor the DES/CuSCN thickness from 60 to 30 nm with increasing spin coating speed, as shown in Figure 3. With decreasing the DES/CuSCN thickness, it is shown that the R_s decreases gradually (Figure 3E), which leads to the remarkable improved FF to 71% for 30 nm thick DES/CuSCN. Meanwhile, the J_{sc} also was improved to 29 mA cm^{-2} with DES/CuSCN thickness of 30 nm compared with the 27.5 mA cm^{-2} of 0 nm CuSCN. The improved J_{sc} with a change of DES/CuSCN thickness is also associated with the Cu concentration and CdSe thickness variation at the front interface in CdSe/CdTe devices, which was confirmed by the EQE measurements later. Thus, the champion device's PCE of 30 nm DES/CuSCN was achieved to be 17.03% with the improved J_{sc}, and *FF*. This device performance is better than our previous CdSe/CdTe device with Cu (4 nm)/Au (40 nm) back contact (PCE ~15%).[32] However, the V_{oc} kept stable, ~0.855 V, with varying the CuSCN thickness, which could be associated with the Cu concentration and may be saturated at 30 nm DES/CuSCN. In addition, it is also observed that the J_{sc} at 30 nm CuSCN shows larger spreading than that of the thicker DES/CuSCN layer, as shown in Figure 3B. This may be due to the nonuniformity of DES/CuSCN coated on the CdTe surface as shown in AFM topography (Figure 2C), the nanocrystalline CuSCN may embed into the back contact and impact the current collection during the *J-V* measurement.

Figure 4A, B shows the *J-V* curve and external quantum efficiency curve for the champion cells with various DES/CuSCN thickness, respectively. The thickness of the DES/CuSCN significantly impacts on the blue response (short wavelengths < 500 nm). Since the CdTe films were experienced in the identical $CdCl_2$ treatment, thus, we assume that the impact of the CdSe window layers impact for the EQE response may not dominate the front interface absorption. However, the different consumption levels of the CdSe window layer post he the $CdCl_2$ treatment, eg, to form the CdSeTe ternary absorber layer, may still be different considering that the nonuniformity of CdTe film, which may impact the front interface transmittance. Here, we focus on the influence of DES/CuSCN thickness on the EQE. The thickness of CuSCN can have two main effects on device performance. First, it determines how much Cu may diffuse into the CdTeSe absorber layer, leading to p-type doping as shown in Figure 4C (Cu poor). Such doping improves the front junction, attributing to the improved V_{oc} and blue response in EQE (Figure 4B). However, too thick CuSCN may result in accumulation of excessive Cu in the front junction regions (Figure 4C, Cu-rich), which is detrimental to device performance. Second, the thickness of CuSCN also determines the conductivity of CuSCN layer, the thicker the DES/CuSCN layer, the lower the conductivity of DES/CuSCN. Therefore, too thick CuSCN would lead to higher series resistance, poorer FF and J_{sc}.

3.3 | NH/CuSCN based CdTe devices

To further reduce the CuSCN thickness, we explore the CdTe device performance using the NH_4OH-based CuSCN. It is successful to achieve 10 and 20 nm thick NH/CuSCN via tuning the rotation speed of NH/CuSCN solution. Figure 5 shows the device performance for the NH/CuSCN in 10 and 20 nm thickness with a comparison to the bare CdTe device. With respect to the CdTe devices without CuSCN, the champion CdSe/CdTe device with 20 nm NH_4OH-based CuSCN can achieve V_{oc} ~0.85 V, J_{sc} ~28.4 mA cm^{-2}, *FF* ~70% and leads to PCE ~16.39%, which is close to to that of the best CdTe device with DES/CuSCN (17.03%). However, the solar cell parameters for the 10 nm NH/CuSCN is lower than that of 20 nm NH/CuSCN. This could be due to the insufficient Cu doping level using this 10 nm thick CuSCN layer. The low Cu concentration impact can also be observed from the improved series resistance and the reduced shunt resistance for this 10 nm thick NH/CuSCN. In addition, the device parameters of

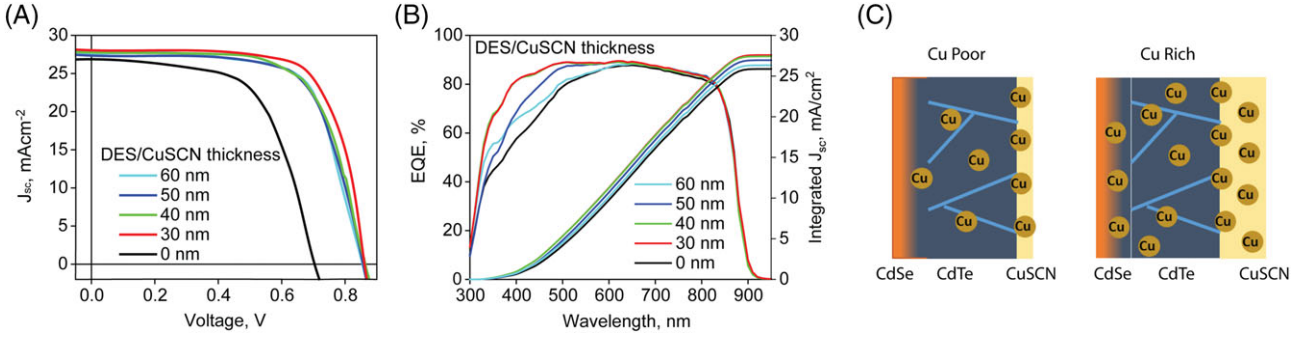

FIGURE 4 A, *J-V* curves and B, external quantum efficiency spectra of the champion CdTe cells with various thicknesses of DES/CuSCN. C, The schematic of the Cu concentration in the CdTe solar cells with varying CuSCN thickness [Colour figure can be viewed at wileyonlinelibrary.com]

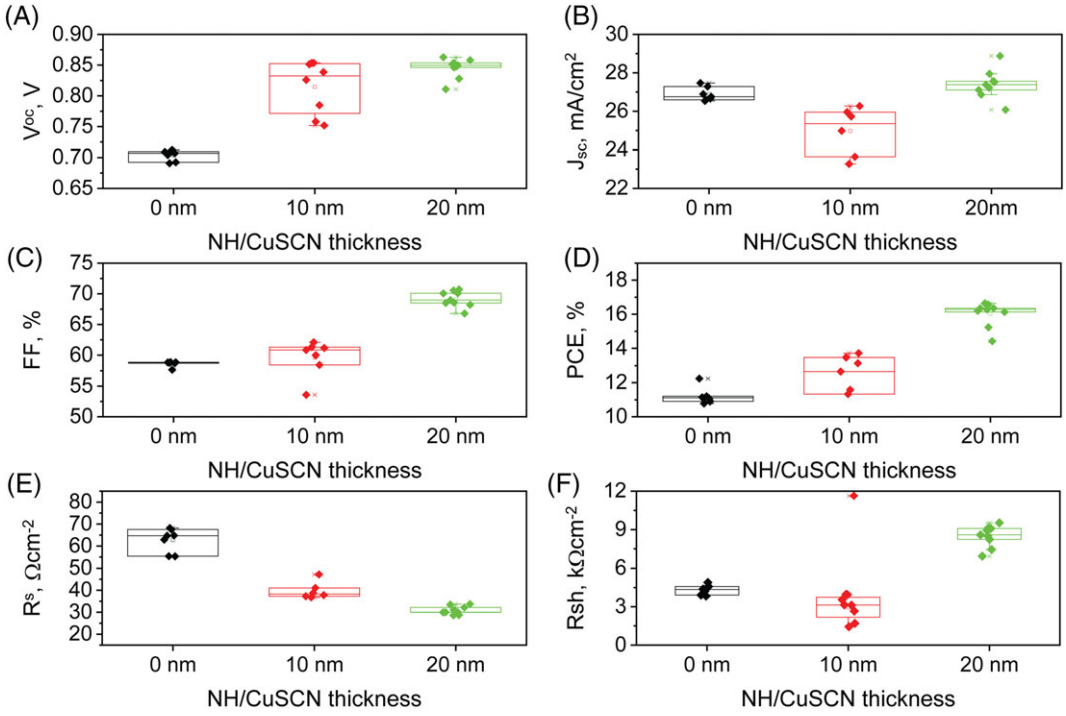

FIGURE 5 Statistical distribution of A, V_{oc}, B, J_{sc}, C, *FF*, D, PCE, E, R_s, and F, R_{sh} of CdTe solar cells based on NH/CuSCN layer. The cell performance data were selected for 10 cells for each NH/CuSCN thickness [Colour figure can be viewed at wileyonlinelibrary.com]

CdSe/CdTe solar cells with thin NH/CuSCN layers show narrow spreading in the R_s and R_{sh}, while more scattering in V_{OC}, FF, and J_{sc}, which could be associated with the thickness dependent resistivity of CuSCN layer, the high roughness of the CdTe film with larger grain size and topographical grain height. For example, 20 nm thick NH/CuSCN could provide sufficient Cu doping but may not provide uniform coverage on the rough CdTe back surface. In contrast, the device parameter of the thicker DES/CuSCN covered CdSe/CdTe devices could provide better surficial coverage, however, the resistivity of thicker CuSCN could impact the R_s and R_{sh} significantly and then impact on the carrier collection.

As shown in Figure 6, both the DES-/CuSCN-coated and NH-/CuSCN-coated CdTe device performance are plotted together for the champion cells. It is demonstrated that both solvents for CuSCN could provide sufficient Cu doping in CdTe with tailoring the thickness of CuSCN to tune the Cu concentration and CuSCN resistivity. Considering the DES more expensive than NH_4OH, it is more desired to use aqueous NH_4OH as a CuSCN solvent. The champion device parameters for DES and NH_4OH solvent-based CuSCN-coated CdTe devices are listed in Table 1, where their V_{oc} is almost identical, while

TABLE 1 Device parameters of champion CdTe cells with CuSCN from DES and NH4OH solvents, respectively

CuSCN Solvent	V_{oc} V	J_{sc} mA cm^{-2}	*FF* %	R_s Ω cm^2	R_{sh} Ω cm^2	PCE %
DES	0.860	28.16	70.31	33.2	10 933	17.03
NH_4OH	0.858	27.65	68.97	33.4	9521	16.36

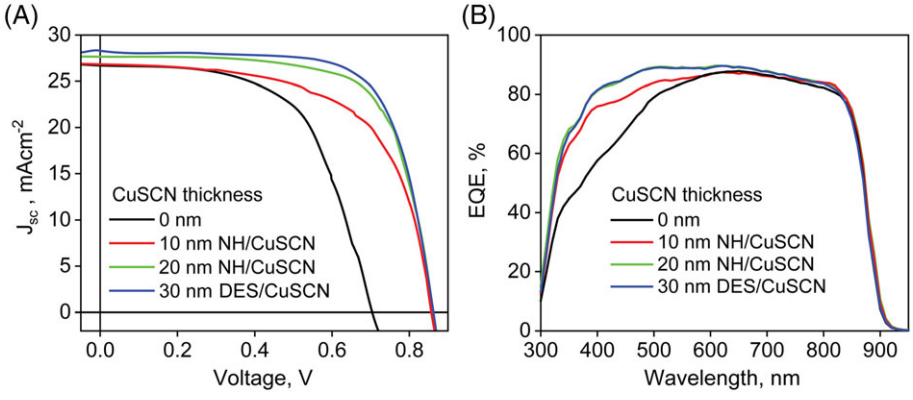

FIGURE 6 A, J-V curves and B, external quantum efficiency spectra of the best performing CdTe cells with NH/CuSCN. The best CdTe device performance with DES/CuSCN is also included for comparison [Colour figure can be viewed at wileyonlinelibrary.com]

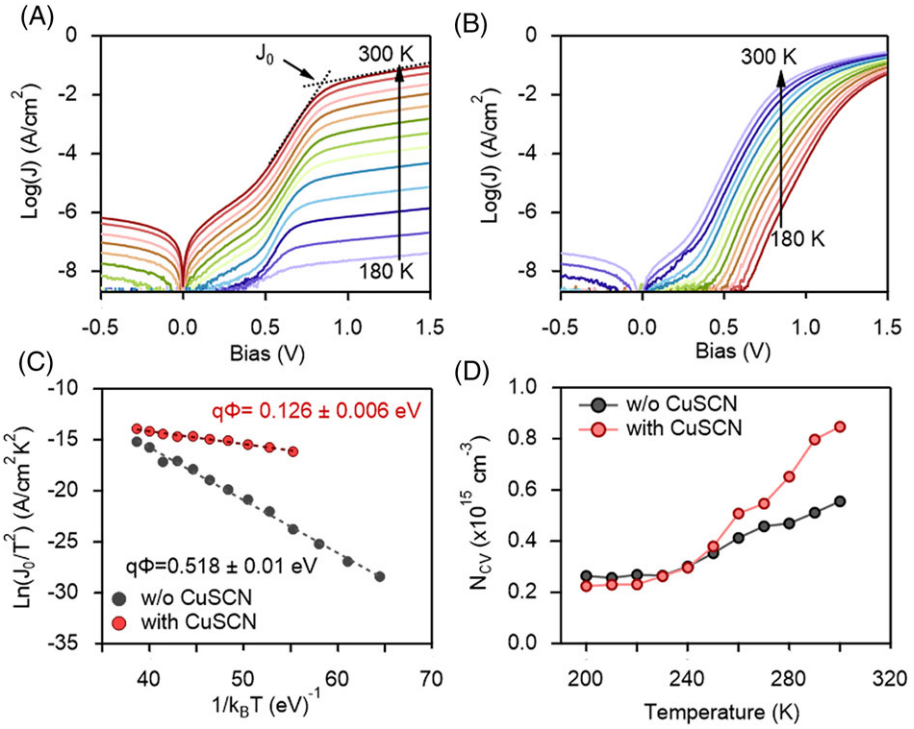

FIGURE 7 Dark J-V-T curves of the CdTe devices A, without and B, with CuSCN layer. C, Arrhenius plots that were used to calculate back-contact barriers (qΦ). D, Carrier concentration as a function of temperature of both devices that are calculated from the fitting curve of Mott-Schottky plots [Colour figure can be viewed at wileyonlinelibrary.com]

the J_{sc} and *FF* for the NH-/CuSCN-coated CdTe device still need to be improved with optimization of the CuSCN thickness and concentration.

3.4 | Hole transport role of solution-processed CuSCN

J-V-T measurements were carried out for CdTe cells with and without CuSCN HTL to understand the effects of CuSCN HTL (Figure 7A, B). J-V diode behaviors were observed from both devices at room temperature. However, cooling the device without CuSCN to lower temperatures led to a rollover at forward biases, indicating non-ohmic contact at the CdTe/back contact interface. However, such rollover is significantly suppressed in the device with CuSCN HTL. We further extracted the activation energy (E_a) for the back-barrier using an Arrhenius plot of $\ln(J_0/T^2)$ versus $1/k_BT$, as shown in the insets of Figure 7C. The back barrier height is measured to be 0.578 eV for the cell without CuSCN, but it is significantly reduced to 0.126 eV for the cell with CuSCN, partially responsible for the improved FF. We further calculated carrier concentration (N_{cv}) based on Mott Schottky plots and C-V-T measurements. As shown in Figure 7D, at room temperature, the hole density in the absorber of the device with CuSCN HTL is higher than in the device without CuSCN HTL. It is reasonable to consider that the increase of hole density is due to Cu diffusion from CuSCN HSL into CdTe layer.

4 | CONCLUSION

In summary, the CdSe/CdTe solar cells integrated with solution-processed CuSCN layer successfully achieved high power conversion efficiency above 16% for both DES and aqueous NH_4OH-based CuSCN. By precisely tuning the CuSCN thickness, the champion cell for the CuSCN can reach 17.03%. The solution-processed CuSCN is a cost-effective method to combine the Cu doping, hole transport, and electron reflecting in CdTe devices. In particular, the aqueous NH_4OH is less toxic and can provide uniform CuSCN layers for highly efficient CdTe devices processed in ambient. This solution-processed CuSCN coating method can significantly reduce the cost of solar energy harvested by CdTe solar module using one step solution-process to realize the Cu doping source, hole extractor, and electron blocker roles.

ORCID

Rasha A. Awni https://orcid.org/0000-0002-5971-0934
Yanfa Yan https://orcid.org/0000-0003-3977-5789
Feng Yan https://orcid.org/0000-0002-0208-6886

REFERENCES

1. Green MA, Hishikawa Y, Dunlop ED, Levi DH, Hohl-Ebinger J, Ho-Baillie AWAY. Solar cell efficiency tables (version 52). *Prog Photovolt Res Appl*. 2018;26(7):427-436.
2. Gloeckler M. Realization of the potential of CdTe thin-film PV. Paper presented at 2016 IEEE 43rd Photovoltaic Specialists Conference (PVSC); 5–10 June 2016, 2016.

3. Next-generation photovoltaics for economical clean energy. 2018; https://phys.org/news/2018-03-next-generation-photovoltaics-economical-energy.html.
4. Ran Fu DF, Margolis R, Woodhouse M, Ardani K. U. S. Solar Photovoltaic System Cost Benchmark: Q1 2017. National Renewable Energy Laboratory Technical Report 2017.
5. Li C, Wu Y, Poplawsky J, et al. Grain-boundary-enhanced carrier collection in CdTe solar cells. *Phys Rev Lett*. 2014;112(15):156103.
6. Zhao Y, Boccard M, Liu S, et al. Monocrystalline CdTe solar cells with open-circuit voltage over 1 V and efficiency of 17%. *Nat Energy*. 2016;1(6):16067.
7. Gloeckler M, Sankin I, Zhao Z. CdTe solar cells at the threshold to 20% efficiency. *IEEE J Photovolt*. 2013;3(4):1389-1393.
8. Ferekides CS, Morel DL. Process development for high Voc CdTe solar cells. United States 2011-05-01 2011.
9. Flores MA, Orellana W, Menéndez-Proupin E. Self-compensation in phosphorus-doped CdTe. *Phys Rev B*. 2017;96(13):134115.
10. Evani V, Khan M, Collins S, Palekis V, Morel D, Ferekides C. Phosphorus doping of polycrystalline CdTe. Paper presented at 2016 IEEE 43rd Photovoltaic Specialists Conference (PVSC); 5–10 June 2016, 2016.
11. Bastola E, Subedi KK, Bhandari KP, Ellingson RJ. Solution-processed nanocrystal based thin films as hole transport materials in cadmium telluride photovoltaics. *MRS Advances*. 2018;3(41):2441-2447.
12. Wen X, Chen C, Lu S, et al. Vapor transport deposition of antimony selenide thin-film solar cells with 7.6% efficiency. *Nat Commun*. 2018;9(1):2179-2179.
13. Luo D, Yang W, Wang Z, et al. Enhanced photovoltage for inverted planar heterojunction perovskite solar cells. *Science*. 2018;360(6396):1442-1446.
14. Guo X, Tan Q, Liu S, et al. High-efficiency solution-processed CdTe nanocrystal solar cells incorporating a novel crosslinkable conjugated polymer as the hole transport layer. *Nano Energy*. 2018;46:150-157.
15. Wolden CA, Abbas A, Li J, et al. The roles of ZnTe buffer layers on CdTe solar cell performance. *Sol Energy Mater Sol Cells*. 2016;147:203-210.
16. Major JD, Phillips LJ, Al Turkestani M, et al. P3HT as a pinhole blocking back contact for CdTe thin film solar cells. *Sol Energy Mater Sol Cells*. 2017;172:1-10.
17. Wang W, Paudel NR, Yan Y, Duarte F, Mount M. PEDOT: PSS as back contact for CdTe solar cells and the effect of PEDOT: PSS conductivity on device performance. *J Mater Sci Mater Electron*. 2016;27(2):1057-1061.
18. Du X, Chen Z, Liu F, et al. Improvement in open-circuit voltage of thin film solar cells from aqueous nanocrystals by interface engineering. *ACS Appl Mater Interfaces*. 2016;8(1):900-907.
19. Wijeyasinghe N, Anthopoulos T. Copper(I) thiocyanate (CuSCN) as a hole-transport material for large-area opto/electronics. *Semicond Sci Tech*. 2015;30(10):104002.
20. Qi YY, Li MG, Wang HL, Zhang W, Chen RF, Huang W. Applications of novel hole-transporting material copper(I) thiocyanate (CuSCN) in optoelectronic devices. *Prog Chem*. 2018;30(6):785-796.
21. Arora N, Dar MI, Hinderhofer A, et al. Perovskite solar cells with CuSCN hole extraction layers yield stabilized efficiencies greater than 20%. *Science*. 2017;358(6364):768-771.
22. Christians JA, Leighton DT, Kamat PV. Rate limiting interfacial hole transfer in Sb2S3 solid-state solar cells. *Energy Environ Sci*. 2014;7(3):1148-1158.
23. Zhao K, Munir R, Yan B, Yang Y, Kim T, Amassian A. Solution-processed inorganic copper(I) thiocyanate (CuSCN) hole transporting layers for efficient p-i-n perovskite solar cells. *J Mater Chem A*. 2015;3(41):20554-20559.
24. Paudel NR, Yan YF. Application of copper thiocyanate for high open-circuit voltages of CdTe solar cells. *Prog Photovolt*. 2016;24(1):94-101.
25. Chaudhary N, Chaudhary R, Kesari JP, Patra A, Chand S. Copper thiocyanate (CuSCN): an efficient solution-processable hole transporting layer in organic solar cells. *J Mater Chem C*. 2015;3(45):11886-11892.
26. Wijeyasinghe N, Regoutz A, Eisner F, et al. Copper(I) thiocyanate (CuSCN) hole-transport layers processed from aqueous precursor solutions and their application in thin-film transistors and highly efficient organic and organometal halide perovskite solar cells. *Adv Funct Mater*. 2017;27(35):1701818.
27. Burgelman M, Nollet P, Degrave S. Modelling polycrystalline semiconductor solar cells. *Thin Solid Films*. 2000;361:527-532.
28. Treat ND, Yaacobi-Gross N, Faber H, et al. Copper thiocyanate: an attractive hole transport/extraction layer for use in organic photovoltaic cells. *Appl Phys Lett*. 2015;107(1):013301.
29. Barnett SA, Blake AJ, Champness NR, Wilson C. Structural isomerism in CuSCN coordination polymers. *Chem Commun*. 2002;15:1640-1641.
30. Perrenoud J, Kranz L, Gretener C, et al. A comprehensive picture of Cu doping in CdTe solar cells. *J Appl Phys*. 2013;114(17):174505.
31. Poplawsky JD, Guo W, Paudel N, et al. Structural and compositional dependence of the CdTexSe1−x alloy layer photoactivity in CdTe-based solar cells. *Nat Commun*. 2016;7(1):12537.
32. Paudel NR, Poplawsky JD, Moore KL, Yan Y. Current enhancement of CdTe-based solar cells. *IEEE J Photovolt*. 2015;5(5):1492-1496.

How to cite this article: Montgomery A, Guo L, Grice C, et al. Solution-processed copper (I) thiocyanate (CuSCN) for highly efficient CdSe/CdTe thin-film solar cells. *Prog Photovolt Res Appl*. 2019;1–8. https://doi.org/10.1002/pip.3136